Materials Science and Engineering A 527 (2010) 3427–3432

Contents lists available at ScienceDirect

Materials Science and Engineering A

journal homepage: www.elsevier.com/locate/msea

Microstructure and mechanical properties of friction stir welded joint of $Zr_{55}Cu_{30}Al_{10}Ni_5$ bulk metallic glass with pure copper

Yufeng Sun, Youngsu Ji, Hidetoshi Fujii*, Kazuhiro Nakata, Kiyoshi Nogi

Joining and Welding Research Institute, Osaka University, Ibaraki 567-0047, Japan

ARTICLE INFO

Article history:
Received 24 September 2009
Received in revised form 29 January 2010
Accepted 25 February 2010

Keywords:
Friction stir welding
Bulk metallic glass
Copper

ABSTRACT

$Zr_{55}Cu_{30}Al_{10}Ni_5$ bulk metallic glass (BMG) plate and pure copper plates with 2 mm in thickness were successfully joined by friction stir butt welding. Microstructure characterization revealed that a clear interface between the two materials was formed in the stir zone and no crystallization from the amorphous phase can be detected. On the copper side in the stir zone, a transitional microstructure of refined elongated grain structure, refined equiaxial grain structure and coarse equiaxial grain structure was found varying with the distance from the BMG/Cu interface. The welded joint showed lower hardness than that of the base metals and finally fractured on the copper side in tensile tests. The ultimate tensile strength of the joint was about 253 MPa, which reached up to 95% of the pure copper.

1. Introduction

Bulk metallic glasses (BMGs) have been attracting great attention due to its unique properties like high strength, large elastic limit and superior corrosion-resist ability, etc. [1–3]. However, BMGs exhibit no global plasticity at ambient temperature and are generally regarded as non-workable and non-weldable materials, which greatly limit its application as engineering materials. Recently, joining of BMGs by various welding methods has been tried one after another in order to widen the practical application of these unique materials. Generally speaking, two kinds of welding methods have been used for the welding of BMGs. One is liquid phase welding method, such as laser welding, electron beam, pulse current, etc. [4–8]. In these methods, the temperature in the nugget is higher than the melting point of work-pieces, which will inevitably induces the crystallization from the amorphous structure or change of chemical composition in the metallic glass. Another kind of welding method is performed in a solid state, which includes friction (stir) welding, explosion welding and diffusion welding, etc. [9–12]. In these methods, the temperature rise is relatively low and an excellent metallurgical joining can be obtained without any crystallization in the BMGs.

Friction stir welding (FSW) is a novel solid state welding method, which is originally invented for the joining of Al and Al alloys. Nowadays, FSW technique has been widely extended and become available for many other metallic materials, such as Cu, Ti, steel and welding of dissimilar materials like Al–Ti, Al–Cu, etc. [13–15]. Comparing with other welding method, FSW process can be accomplished far below the melting point of the work-pieces, which shows a strong candidate for the joining of BMGs or BMG to other crystalline materials. For example, Ji et al. has successfully friction stir welded two Zr-base BMG plates together without crystallization and defects in the stir zone by using a rotation tool with large shoulder [16]. Ma et al. first applied FSW to the joining of $Zr_{55}Cu_{30}Al_{10}Ni_5$ BMG with AlZnMgCu alloys, which shows strong bonding and mixed microstructure with BMG particles in the stir zone [17]. More recently, Qin et al. prepared $Zr_{55}Cu_{30}Al_{10}Ni_5$ BMG joint with crystalline Al using FSW technique [18]. Up to now, no other metallic materials have been reported to be joined with BMGs by means of FSW method.

In this study, a $Zr_{55}Cu_{30}Al_{10}Ni_5$ BMG and commercial pure copper were subjected to FSW process to investigate the weldability of these dissimilar materials. Since the aluminum alloys have a low melting point and the temperature rise during the FSW process was said to be lower than the onset crystallization temperature (T_x) of $Zr_{55}Cu_{30}Al_{10}Ni_5$ BMG, the FSW of copper with the $Zr_{55}Cu_{30}Al_{10}Ni_5$ BMG is relatively more difficult due to its higher melting point. After FSW of $Zr_{55}Cu_{30}Al_{10}Ni_5$ BMG with pure copper, the microstructure evolution and the mechanical properties of the welded joint were investigated and discussed.

2. Experimental procedure

Plates of $Zr_{55}Cu_{30}Al_{10}Ni_5$ BMG with 2 mm in thickness were prepared by injection cast into water-cooled copper mould in an induction melting furnace. The copper plates were as-received in

* Corresponding author. Tel.: +81 6 68798663; fax: +81 6 68798663.
E-mail address: fujii@jwri.osaka-u.ac.jp (H. Fujii).

0921-5093/$ – see front matter © 2010 Elsevier B.V. All rights reserved.
doi:10.1016/j.msea.2010.02.072

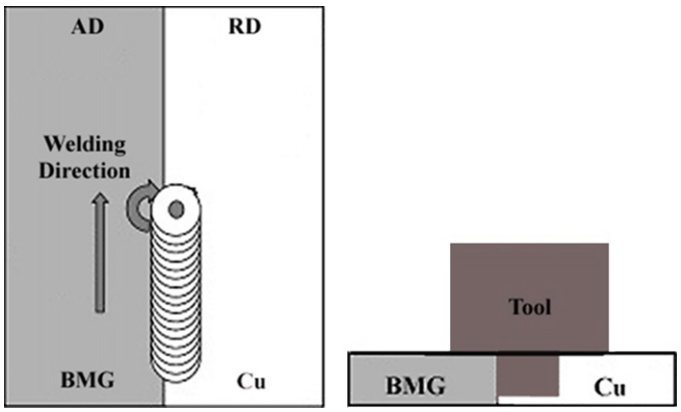

Fig. 1. Schematic illustration showing the tool and work-piece positions during the FSW process.

1/2H state with average grain size, Vickers hardness and tensile strength of about 20 μm, 90 HV and 266 MPa, respectively. Then the BMG plates were friction stir butt welded with 2 mm thick commercial pure copper at a welding speed of 100 mm/min and a tool rotation speed of 400 rpm. The coated WC tools were used, which had a shoulder of 12 mm in diameter and a cylindrical probe of 4 mm in diameter and 2 mm in length. During the FSW process, the BMG was put on the advancing side and the pure copper on the retreating side. The tool probe was offset into the pure copper side with the lateral surface of the probe slightly touching the BMG side. Fig. 1 shows the details of the tool and work-piece positions during the welding process.

After welding, the cross-section of the stir zone perpendicular to the welding direction was cut off for microstructural characterization by optical microscopy (OM), electron back-scattering diffraction (EBSD) and transmission electron microscopy (TEM). The EBSD measurements were carried out using a program developed by TSL (OIM-Analysis 5.0) in a JSM 5200 SEM operated at 20 kV. Thin foils with about 100 nm in thickness were prepared by using a Hitachi FB-2000S focused ion beam (FIB) instrument and were observed in a Hitachi 800 TEM to investigate the BMG/Cu interface structure. The phase constitution of the BMG/Cu interface was detected by X-ray diffraction (XRD) with a micro-area Bruker D8 Discover X-ray Diffractometer. The hardness profile was measured along the center line of the cross-section with an applied load of 980 mN and dwell time of 10 s. At least three rectangle tensile specimens were machined perpendicular to the welding direction with the stir zone located in the center of the specimen. The tensile tests were carried out with an Instron 5500R machine at a cross-head speed of 1 mm/min.

3. Experimental results

Fig. 2 presents the OM images showing the cross-sectional microstructure of the FSW BMG/Cu joint. From Fig. 2(a), a clear interface can be observed in the stir zone so that the two different materials can be easily distinguished, namely the BMG on the left side and pure copper on the right side of the interface. No weld defects like grooves or cavities can be detected within the entire stir zone, indicating that a sound welding was obtained between the BMG and pure copper by FSW. Compared with the previous FSW of BMG-7075 Al joint, in which a mixed area consisting of BMG particles and aluminum alloy formed due to the intense deformation [17], no such a mixed area can be observed in the FSW BMG/Cu joint due to the slight touching of the rotating tools with BMG side during the welding process. However, some BMG fragments with irregular shapes and different sizes can still be found distributed in the copper side. All the BMG fragments with size less than 100 μm and most of the blocky BMG fragments with size larger than 100 μm formed a clear interface with the copper matrix, which were shown in Fig. 2(b) and (c) as typical examples. While for some blocky BMG fragments, some micro-voids can be observed and was indicated by a black arrow in Fig. 2(d). The formation of the micro-voids might be caused by the irregular shape of the blocky BMG fragments. The out of flatness of the BMG surface cannot be completely contacted and filled with copper materials even by intense stirring during the welding process.

Fig. 3 shows the XRD patterns measured at the BMG/Cu interface in the stir zone. The XRD curve exhibits a superimposition of several sharp peaks characteristic for crystalline phase on a broad halo peak from the amorphous phase, indicating the existence of a mixture of the amorphous and some crystalline phases. After indexing, the position and the intensity of the sharp crystalline peaks match exactly with that of pure copper. No other phases can be detected within the sensitivity limit of XRD. This result indicates that neither chemical reaction between the two materials nor crystallization from the amorphous phase took place during the entire FSW process.

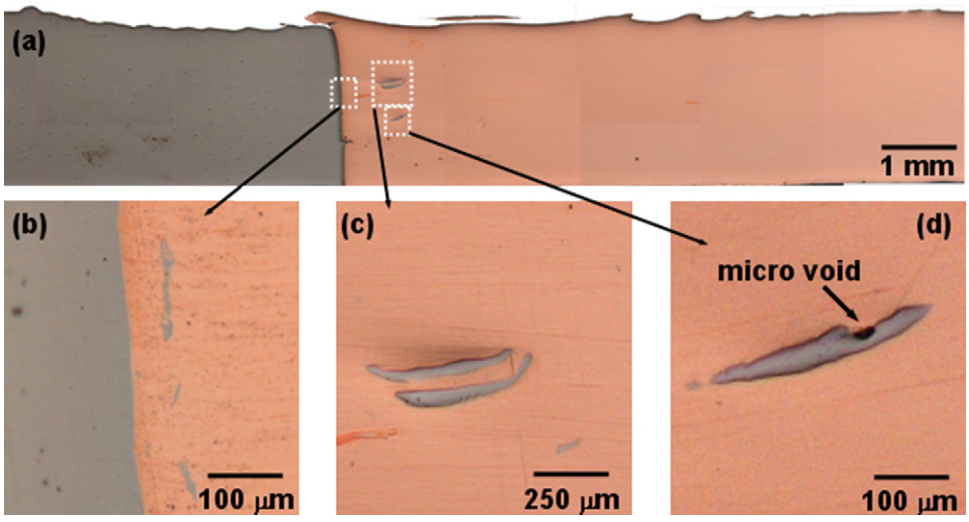

Fig. 2. OM images showing the (a) cross-sectional macrostructure of the stir zone perpendicular to the welding direction, (b) small and (c) blocky BMG fragments with smooth surface, and (d) blocky BMG fragments with micro-void.

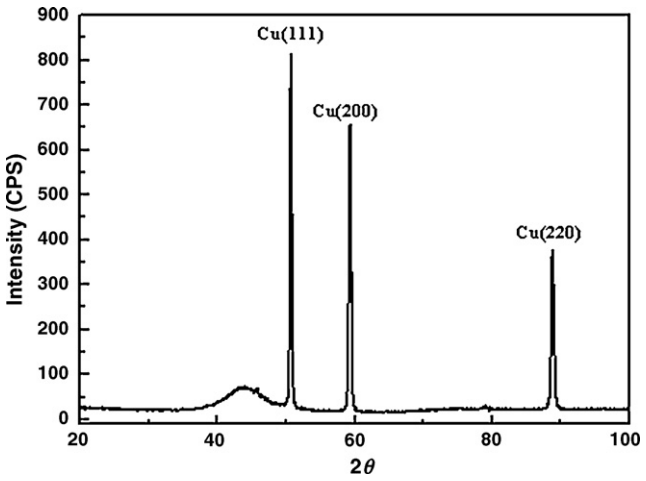

Fig. 3. XRD curve measured at the interface between the BMG and the copper plate.

Fig. 4 shows the EBSD orientation map obtained along the BMG/Cu interface of the FSW processed sample. The enclosed rectangle area indicated in Fig. 4(a) was scanned for EBSD measurement, which included a small area of BMG and the copper plate in the joint. At the same time, some BMG fragments can be found emerged from the copper plates because the copper was electropolished when preparing the EBSD samples. In the EBSD maps shown in Fig. 4(b), the black area on the left side indicated the BMG side, because no Kikuchi pattern can be obtained from the BMG due to its disordered atomic configuration. The right side is the copper plate, which shows equiaxial structure from the EBSD observation. It was found that the copper close to the BMG/Cu interface revealed a very refined equiaxial grain structure. However, when departing from the interface, the microstructure became coarse and the grain size of the copper gradually increased to about 10 μm, although it is still smaller than that of the copper base metal. In addition, a few abnormally grown grains can also be observed. This refined microstructure with smaller grain size in the stir zone after FSW process is common for the FSW processed metallic materials and generally is believed to be caused by the dynamical recrystallization of the highly deformed grains [19].

Fig. 5 shows the TEM image revealing the detailed microstructure of BMG/copper interface in the welded joint. Similar with the morphology in the OM image in Fig. 2(a), a clear interface without any intermetallic compounds can be found between the different materials, namely the BMG side in the left and copper side in the right. The BMG side still keeps its homogeneously amorphous structure, which can be confirmed by the corresponding selective area electron diffraction (SAED) pattern inserted in the left bottom corner in Fig. 5. While on the copper side, a transitional microstructure from elongated to equiaxial grain structure formed when departing from the BMG/Cu interface. The elongated copper grains distributed parallel with the BMG/copper interface, together with some gray strips with no contrast inside. The gray strips can be identified as metallic glass by the broaden diffraction ring pattern inserted in the right upper corner in Fig. 5. It seemed that the elongated copper grains were formed by extrusion between the rotating probe and the hard BMG plate. On the other hand, it was known that the materials in the stir zone are shear deformed by the rotation tools and the materials near the tool edge are generally elongated to accommodate the geometric strain in the stir zone. Simultaneously, the strips of the metallic glass were stripped off from the BMGs by the rotating probe during the welding process and the distribution of the BMG strips will certainly restrict the recrystallization of the deformed copper grains. The elongated grain area is very small and was not detected by the EBSD measurements. What is more, the mixture of BMG strips also reduced the quality of the diffraction pattern and increased the difficulties of phase indexing. Beyond the elongated grain area, the microstructure is dominated by equiaxial copper grains with average grain size of 500 nm, which corresponds to the refined equiaxial structure in the EBSD observation shown in Fig. 4(b). Combined with the EBSD and TEM observation, the microstructural evolution on copper side can be therefore understood and illustrated in Fig. 5. That is, elongated grain structure formed close to the BMG/Cu interface. With the increasing distance from the interface, the microstructure changed into refined

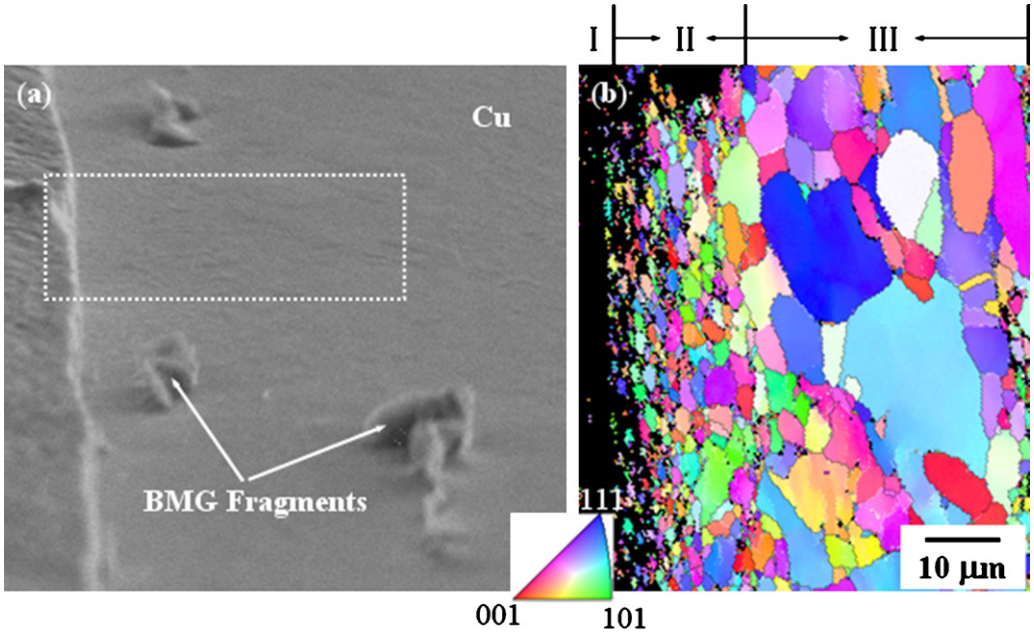

Fig. 4. (a) SEM images showing the area for EBSD measurements and (b) EBSD map obtained at the interface between the BMG and the Cu plate (I, BMG area; II, refined equiaxial area; III, coarse equiaxial area).

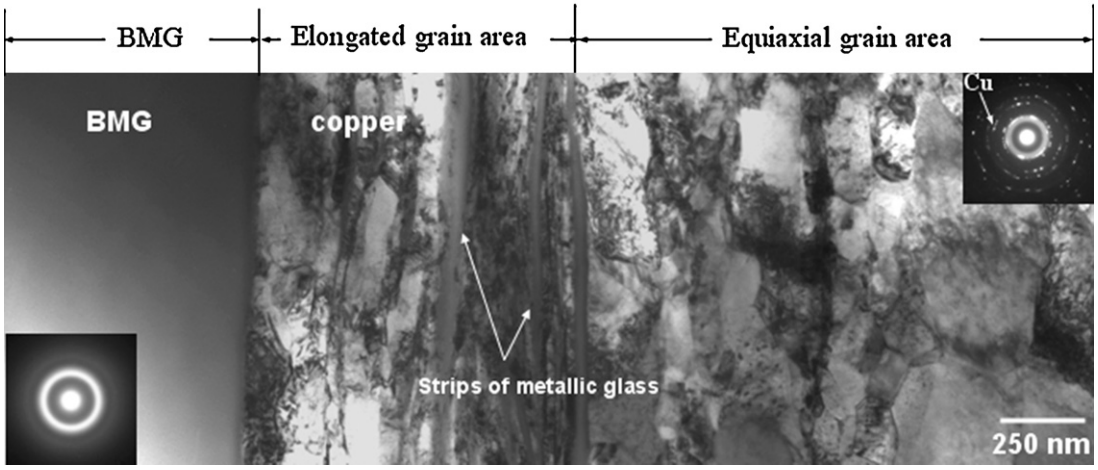

Fig. 5. TEM image showing the microstructural transition across the BMG/Cu interface.

equiaxial grain structure and finally become coarse equiaxial grain structure.

Fig. 6 shows the TEM images of the microstructure of copper side in the stir zone, in which a large BMG particle was found embedded in the copper matrix. The BMG particle has a generally smooth surface and still remains its amorphous structure. No transition layer or reaction layer was found at the BMG/Cu interface.

Fig. 7 shows the hardness profile of the stir zone across the BMG/Cu interface. The zero position denotes the interface between the two different materials. On the left side to the zero position, the hardness is about 545 HV, which exhibits the intrinsic high strength of BMGs. However, the hardness suddenly drops down to 80 Hv around the zero position, i.e., the BMG/Cu interface. While in the stir zone away from the interface, the average hardness decreased further to about 70 Hv. Obviously, the hardness value in the stir zone is lower than that in base copper metal, even though the grain size is a little smaller in the stir zone. This phenomenon of low hardness in smaller grain size has been recently reported in the FSW of pure Cu. For example, Ma et al. found that the average grain size was decreased to 9 μm in the stir zone from 18 μm in the base metal, while the hardness fell from 82.2 Hv in the base metals down to 72.8 Hv in the stir zone. Lee also found that the hardness of the FSW processed pure copper is lower in the stir zone than in the base metal, although the microstructure in the stir zone is much refined due to the dynamic recrystallization. According to their explanation, the reduced hardness was resulted from that the annealing softening effect is larger than the strain hardening effect after friction stir welding [19,20].

The tensile tests were carried out to evaluate the mechanical properties of the BMG/Cu joint. Three strain–stress curves were shown in Fig. 8 as a typical example. The strain–stress curves were moved from their original position for clarity. From the curves, the ultimate tensile strengths of the welded specimen are similar after each test and ranged from 240 to 253 MPa, which is a little lower than 266 MPa of the pure copper used in this study. That is, the ultimate tensile strength of the BMG/Cu welded joint can reach from 90% to 95% of the base pure copper. From the appearance of two fractured sample inserted in Fig. 8 as typical examples, the tensile specimen usually fractured on the copper side in the stir zone, however, very close to the BMG/Cu interface. The locations of the fracture on one hand confirmed that the bonding of the BMG/Cu interface was excellent and stronger than the stir zone. On the other hand, it indicated that the BMG fragments embedded in the copper matrix will deteriorate the mechanical properties of the joints. Because from the microstructure observation, it can be known

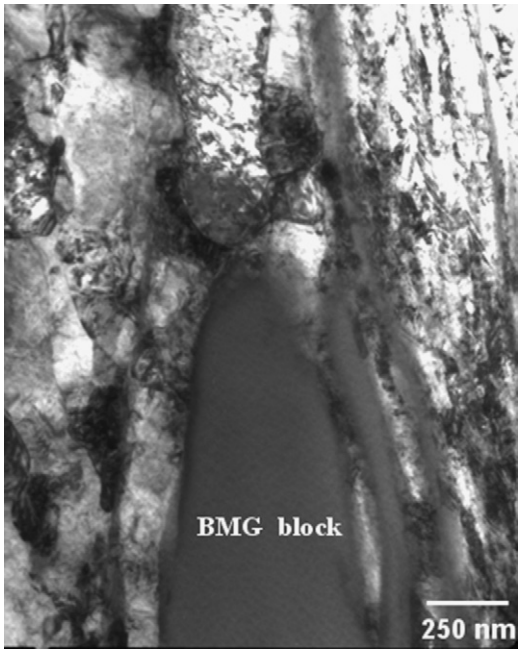

Fig. 6. TEM image showing that the metallic glassy block mixed into the Cu part.

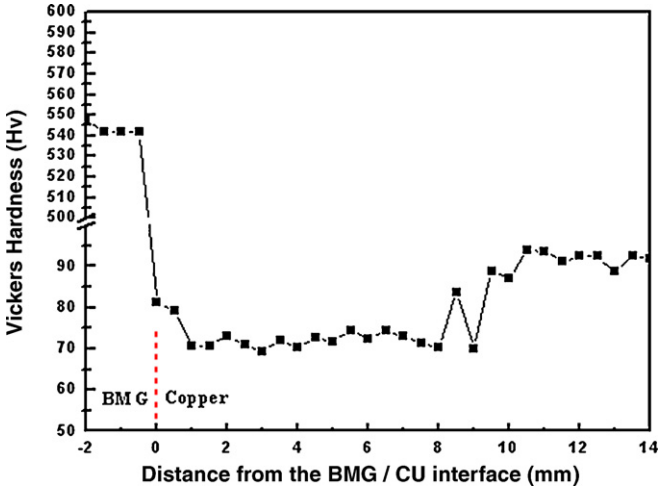

Fig. 7. Hardness profile in the stir zone across the BMG/copper interface.

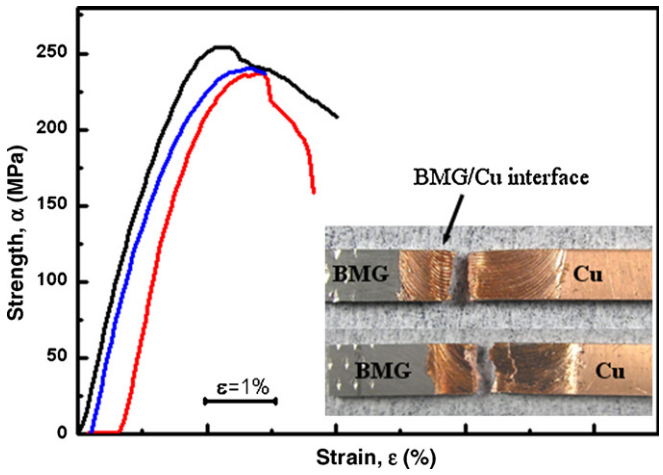

Fig. 8. Tensile strain–stress curve of the BMG/Cu joint with the fractured specimen inserted.

that BMG fragments generally distributed close to the fracture locations.

Fig. 9 shows the SEM image of the fracture surface of the joint after tensile tests. From the macro-view of the fractured plane as shown in Fig. 9(a), no obvious BMG particles or fragments can be observed. However, from the SEM images at high magnification, some BMG particles as indicated by arrows in Fig. 9(b) and some strip-like BMG fragments as indicated by arrows in Fig. 9(c) can be observed. It confirmed that the location where the BMG fragments aggregated is the weak place in the BMG/Cu welded joint.

4. Discussion

During FSW, the materials for welding undergo a high strain and high strain rate process, accompany with the local temperature rise generated by the friction between the tool and work-piece. This kind of severe plastic deformation is necessary for the joining of conventional crystalline materials like Al, Cu, Ti and Mg alloys, etc. However, the plastic deformation or high temperature will inevitably bring risks of brittle failure or crystallization to the BMGs. As a kind of metastable metallic materials, BMG may transform to a stable state with reduced total free energy through crystallization from the amorphous structure if the BMGs were exposed in the supercooled liquid region for long time or at temperature higher than T_x [21,22]. In the previous FSW of BMG to 7075 Al alloys, the temperature rises in both BMG side and 7075 Al side during the welding process were said to be higher than the onset glass transition temperature (T_g) but less than T_x of the $Zr_{55}Cu_{30}Al_{10}Ni_5$ BMG [17]. Therefore, the BMG was supposed to be deformed in the supercooled liquid region and the viscous flow of the BMG would benefit its mixing with 7075 Al alloy, without formation of defects and crystallization from the BMG. However, pure copper has a melting point higher than aluminum alloys, which indicates that higher temperature rise is necessary for the FSW of pure copper. By using the same machine, the peak temperature for FSW of pure copper was measured between 480 and 612 °C, higher than the T_x of $Zr_{55}Cu_{30}Al_{10}Ni_5$ BMG [23]. The high temperature rise provides thermodynamic preference for the crystallization from the amorphous structure. However, the nucleation of a crystalline phase is a time-depended process and an incubation period is necessary before the occurrence of crystallization from the amorphous structure. It was reported that the incubation time of crystallization from $Zr_{55}Cu_{30}Al_{10}Ni_5$ BMG is about 1 min at 500 °C [24]. According to the temperature and thermal history for the FSW of pure copper, the local temperature in the stir zone drops sharply from its peak temperature, i.e., 612 °C, down to 500 °C within a couple of seconds due to the excellent thermal conductivity of pure copper and the rapid moving of the tools along the welding direction. As a result, the thermally induced crystallization of the Zr-based BMG can be avoided.

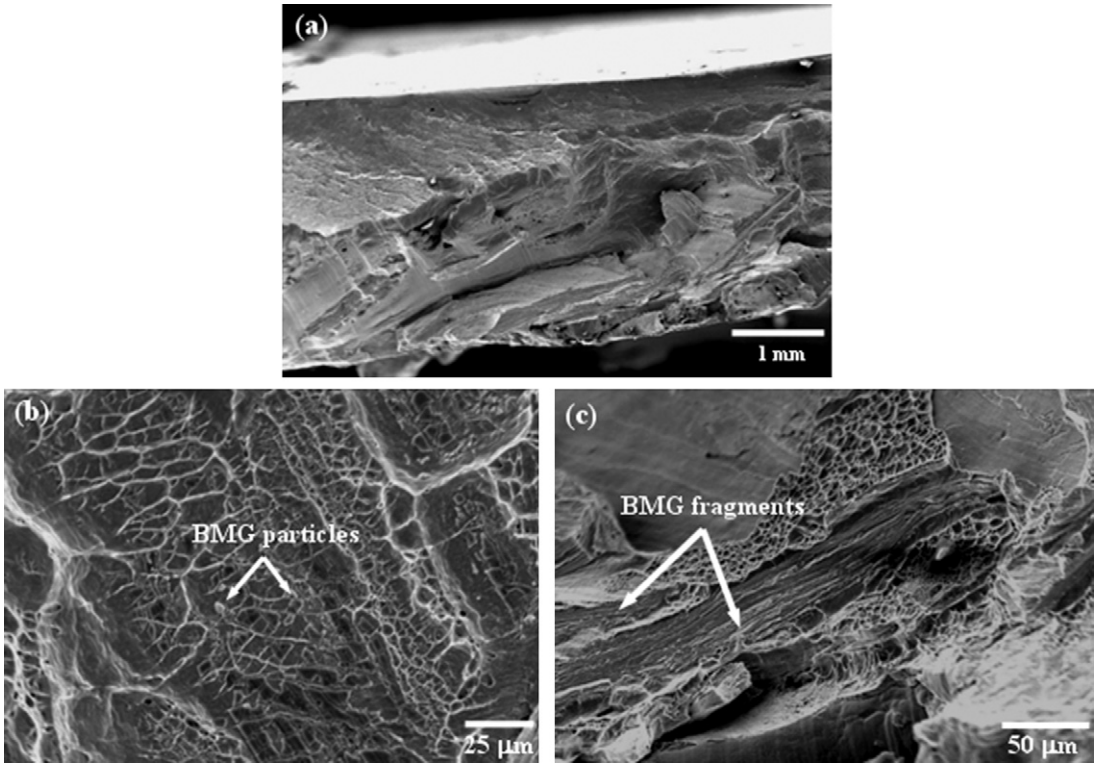

Fig. 9. SEM images showing the tensile fracture surfaces of the BMG/copper joint (a) macro-view of the fracture surface; (b) magnified view showing the BMG particles on the fractured plane; (c) magnified view showing the strip-like BMG fragments on the fractured plane.

The crystallization of BMG can also be induced by plastic deformation. It has been reported that substantial structure rearrangements can take place within the shear bands of metallic glasses after plastic deformation at room temperature [25–27]. However, the stress flow of BMG changes to homogeneous flow at temperature higher than T_g from the inhomogeneous flow at low temperature. If crystallization occurred when deformed at supercooled liquid region, it was generally regarded as a result of annealing effect caused by long time exposure at high temperature. While the plastic deformation induced crystallization is not obvious. According to the previous study of friction stir processing (FSP) of Zr-based BMG, no crystallization but only nanoscale structure bands were observed. It also indicates that crystallization can be avoided during the severe plastic deformation process, like FSP. In the present study, no signs of crystallization can be found in the stir zone. However, whether the surrounded copper matrix may restrict the crystallization of BMG at high temperature or not is still uncertain.

After welding, the mechanical properties of the welded joints can be affected by either the microstructure refinement or the embedded BMG fragments in the copper matrix. However, the microstructure refinement of copper in the stir zone is not expected to improve the mechanical properties. The annealing soft effect of copper will decrease the tensile strength, which shows the same phenomena as that in the hardness tests. In addition, we found that blocky BMG fragments would fracture from the BMG plate and would be mixed with copper in the stir zone if the rotations tools were moved into the BMG side. As a result, voids usually formed between the BMG blocks and the copper matrix due to the different volume shrinkage when cooled from the high temperature. The formation of void will decrease the mechanical properties of the joint and lead to early fracture of the materials. To prevent these problems, the rotation tools were often moved to the crystalline materials side during the welding process to reduce the intense interaction between the tools and the BMGs. The BMG fragments embedded in the copper matrix was supposed to have two aspects on the mechanical properties of the welded joints. The presence of the BMG fragments retarded the recrystallization of the deformed Cu grains and finally refined the microstructure nearby, which will contribute to the improved mechanical properties. On the other hand, the possible formation of micro-void around the BMG fragments might split the continuity of the matrix and act as the source of the crack growth, which will result in the early fracture of the materials. In this present study, the BMG plate is slightly touched with the rotation tools and only small pieces of BMGs can be strip off and stirred into the copper side, which will greatly reduce the formation of voids around the BMG fragments. As a result, the tensile strength of the welded joint is high and can reach 90–95% of the copper base metal.

5. Conclusions

In this paper, the $Zr_{55}Cu_{30}Al_{10}Ni_5$ BMG plates were successfully friction stir welded to pure copper plates to form a defect-free joint. The conclusions can be drawn from the above descriptions and shown as below:

1. After welding, a straight and clear interface formed between the two dissimilar materials due to slightly touching the BMG side by the rotation tools. No chemical reaction and crystallization from the BMG can be detected at the interface and within the stir zone.
2. From the BMG/Cu interface to the copper side in the stir zone, a transitional microstructure changed from elongated grain structure to refined equiaxial grained structure and finally became coarse grain structure.
3. The bonding of the BMG and pure copper by FSW is strong and the strength of the FSW processed BMG/Cu joint can reach up to 95% of the pure copper.

Acknowledgements

The authors wish to acknowledge the financial support of a Grant-in-Aid for the Cooperative Research Project of Nationwide Joint-Use Research Institutes, the Global COE Programs from the Ministry of Education, Sports, Culture, Science, a Grant-in-Aid for Science Research from the Japan Society for Promotion of Science and Technology of Japan, Toray Science Foundation, ISIJ Research Promotion Grant, and Iketani Foundation.

References

[1] W.H. Wang, C. Dong, C.H. Shek, Mater. Sci. Eng. R 44 (2004) 45–89.
[2] A. Inoue, Acta Mater. 48 (2000) 279–306.
[3] W.L. Johnson, MRS Bull. 24 (1999) 42–56.
[4] J. Kim, Y. Kawamura, Scr. Mater. 56 (2007) 709–712.
[5] Y. Kawamura, S. Kagao, Y. Ohno, Mater. Trans. 42 (2001) 2649.
[6] Y. Kawamura, Y. Ohno, Mater. Trans. 42 (2001) 717.
[7] Y. Kawamura, Y. Ohno, Scr. Mater. 41 (2001) 127.
[8] T. Kuroda, K. Ikeuchi, M. Shimada, A. Kobayashi, et al., Mater. Trans. 50 (2009) 1259–1262.
[9] C.H. Wong, C.H. Shek, Scr. Mater. 49 (2003) 393–397.
[10] K.X. Liu, W.D. Liu, J.T. Wang, et al., Appl. Phys. Lett. 93 (2008) 081918.
[11] H.S. Shin, H.Y. Choi, J.S. Park, Rev. Adv. Mater. Sci. 18 (2008) 104–106.
[12] H.S. Shi, Y.J. Jeong, H.Y. Choi, J. Alloys Compd. 434 (2007) 102–105.
[13] R. Nandan, T. Debroy, H.K.D.H. Bhadeshia, Prog. Mater. Sci. 53 (2008) 980–1023.
[14] Y.S. Sato, S.H.C. Park, M. Michiuchi, H. Kokawa, Scr. Mater. 50 (2004) 1233–1236.
[15] Y.S. Sato, M. Urata, H. Kokawa, et al., Mater. Sci. Eng. A354 (2003) 298–305.
[16] Y.S. Ji, H. Fujii, Y.F. Sun, et al., Mater. Trans. 50 (2009) 1300–1303.
[17] D. Wang, B.L. Xiao, Z.Y. Ma, H.F. Zhang, Scr. Mater. 60 (2009) 112–115.
[18] Z.X. Qin, C.H. Li, H.F. Zhang, et al., J. Mater. Sci. Technol. 25 (2009) 853–856.
[19] G.M. Xie, Z.Y. Ma, L. Geng, Scr. Mater. 57 (2007) 73–76.
[20] W.B. Lee, S.B. Jung, Mater. Lett. 58 (2004) 1041–1046.
[21] Y.L. Gao, J. Shen, J.F. Sun, et al., Mater. Lett. 57 (2003) 1894–1898.
[22] L. Liu, K.C. Chan, T. Zhang, J. Alloys Compd. 396 (2005) 114–121.
[23] Y. Takada, Friction stir welding of Ultrafine grained materials, Master Thesis, Osaka University, 2005.
[24] Y.L. Gao, J. Shen, J.F. Sun, G. Wang, et al., Mater. Lett. 57 (2003) 1894–1898.
[25] C.A. Pampillo, H.S. Chen, Mater. Sci. Eng. 13 (1974) 181.
[26] C.A. Pampillo, J. Mater. Sci. 10 (1975) 1194.
[27] P.E. Donovan, W.M. Stobbs, Acta Metall. 29 (1981) 1419.